Hindawi
International Journal of Antennas and Propagation
Volume 2023, Article ID 5574730, 12 pages
https://doi.org/10.1155/2023/5574730

Research Article

Research on Reradiation Interference Resonance Mechanism of Power Transmission Lines in Medium-Wave Band Based on Characteristic Mode Theory

Bo Tang,[1,2] Feng Wang ,[1] Jiangong Zhang,[3] Ren Liu,[1] and Zhibin Zhao[4]

[1]*College of Electrical Engineering and New Energy, China Three Gorges University, Yichang 443002, China*
[2]*Hubei Provincial Engineering Technology Research Center for Power Transmission Line, Yichang 443002, China*
[3]*China Electric Power Research Institute, Wuhan 430073, China*
[4]*College of Electrical and Electronic Engineering, North China Electric Power University, Beijing 100096, China*

Correspondence should be addressed to Feng Wang; wf20160@ctgu.edu.cn

Received 23 February 2023; Revised 23 March 2023; Accepted 24 April 2023; Published 2 May 2023

Academic Editor: Sreenath Reddy Thummaluru

The key to decreasing reradiation interference (RRI) of power transmission lines on adjacent radio stations is to clarify the RRI resonance mechanism. Aiming at the defects of existing RRI resonance analysis methods, including frequency limitation and lack of physical explanation, a RRI resonance analysis method based on characteristic mode (CM) theory is proposed in this paper. Firstly, based on the generalized eigenvalue equation, a set of characteristic currents with orthogonal relationship and their eigenvalues for power transmission lines are solved, and combined with Poynting's theorem, the CM radiation characteristics are analyzed. Secondly, under specific external excitation, CM-related parameters are obtained through modal decomposition. Finally, the total energy radiated by power transmission lines is decomposed into the superposition of energy radiated by each CM, and the mechanism of RRI resonance is clarified from the perspective of CM. The simulation results show that compared with the IEEE guide and the generalized resonance theory, the method in this paper is effective and independent of observation points, which can provide a theoretical support for further research on the RRI suppression measures.

1. Introduction

There exists a unique electromagnetic scattering resonance phenomenon of RRI caused by power transmission lines on neighboring radio stations [1–3]. This phenomenon makes it difficult to accurately measure and effectively suppress RRI. As a result, the protection distance between power transmission lines and radio stations can only be determined by the spatial attenuation characteristics of the maximum interference value, which may lead to excessive redundancy of the protection distance, and even the adjacent communication facilities cannot work normally. Therefore, in order to seek specific RRI suppression measures, it is necessary to clarify the RRI resonance mechanism of power transmission lines.

In 1996, IEEE summarized the research work on RRI from power transmission lines to AM radio stations and formulated a technical guide [4]. In this guide, the complex tower is equivalent to a single cylindrical conductor [5, 6], so IEEE explains the resonance phenomenon of RRI below 1.7 MHz by the antenna theory. When the tower is insulated with the ground wire, the tower and its ground image can be equivalent to a half-wave antenna, and resonance occurs when the height of the tower is a quarter wavelength of the incident electromagnetic wave; when the tower is connected to the ground wire, the two adjacent towers, the ground wire, and their ground images form a loop, which can be equivalent to a ring antenna. When the length of the loop is an integer multiple of the wavelength, resonance occurs [4]. However, the premise of IEEE guide is that the tower can be equivalent to a single wire antenna. When the frequency exceeds 1.7 MHz, the electrical size of the complex truss structure of the tower cannot be ignored relative to the wavelength [7], that is, the tower cannot be equivalent to a single wire antenna, and new theories and methods must be introduced to explain the interference resonance phenomenon.

Due to the large-scale construction of ultra-high-voltage projects in China, the researchers mainly focus on the rapid solution of the RRI of power transmission lines, trying to establish the protection distance standards between ultra-high-voltage power transmission lines and various radio stations for RRI [2, 8–11]. The key to solving the protection distance is to obtain the maximum value of RRI. During the research, the resonant frequency is selected according to the IEEE guide, or some frequency points in the interval are selected to calculate the maximum RRI [9]. However, when the resonant frequency is unpredictable, method of simply analyzing the change of electric field at individual frequency points may cause redundant protection distance [2]. For this reason, researchers in China have gradually carried out a further study of RRI resonance.

Different from the antenna theory adopted in the IEEE guide, which equates power transmission lines as antennas, the electromagnetic open system composed of radio stations and power transmission lines in wide-area space is equivalent to a generalized electromagnetic closed system from the perspective of complex power balance [3, 12, 13]. Then, the generalized resonance theory [14] is introduced, and the electric field intensity resonance of RRI is transformed into a study of the quality factor Q value of the electromagnetic open system. Through this method, the predicted resonant frequency of RRI is extended to 3 MHz [3]. However, since the generalized resonance theory takes the whole electromagnetic system as a research target, it ignores the correlation mechanism between the structure and scattering characteristics of power transmission lines. As a result, this method can only provide very limited physical interpretation for the electromagnetic radiation mechanism of power transmission lines.

In recent years, in antenna engineering, a numerical analysis method that can analyze the intrinsic electromagnetic characteristics of antenna structures, namely, the CM theory [15–18], has attracted wide attention. This method decomposes the total scattering response of the target into the superposition of the mode response, and the intrinsic characteristics of the electromagnetic problem of the target can be described by orthogonal modes [19–22]. Therefore, if combining with the antenna theory of RRI studied by IEEE [4], the metal components of power transmission lines can be equivalent to large-scale complex antenna components under the excitation of external electromagnetic wave, and then the electromagnetic characteristics of power transmission lines can be studied by using CM theory, which can provide a new idea for the research on RRI resonance mechanism of power transmission lines.

In order to clarify the RRI resonance mechanism in the medium-wave band, this paper proposes a RRI resonance analysis method based on CM theory. Through mathematical operators and energy relationships, a set of energy decoupling CMs for power transmission lines is defined, and the total energy radiated by power transmission lines is decomposed into the superposition of the energy radiated by each CM. Then, by using the CM-related parameters, we analyzed the CMs that mainly contribute to the total energy radiated by power transmission lines, and the RRI resonance mechanism is cleared from the perspective of CM.

2. The Phenomenon of RRI Resonance and Its Explanation

2.1. Resonance Phenomenon of RRI. The distance between high-voltage power transmission lines and a radio station is usually several kilometers. Considering that radio stations usually work at frequencies as high as megahertz, RRI can be regarded as the electromagnetic scattering caused by metal structures of power transmission lines under the irradiation of plane waves. The mathematical model is shown in Figure 1.

Under the irradiation of incident electromagnetic wave $\mathbf{E}_i(\mathbf{r}')$ (incident direction is (θ_i, φ_i)), induced current $\mathbf{J}(\mathbf{r}')$ is generated at $\mathbf{r}'$ (the surface of metal structure of power transmission lines), and $\mathbf{J}(\mathbf{r}')$ is denoted by the vertical lines under "induced current" in Figure 1. Also, $\mathbf{J}(\mathbf{r}')$ can be seen as a new field source with the same frequency of $\mathbf{E}_\mathrm{i}(\mathbf{r}')$, and this field source will radiate electromagnetic waves $\mathbf{E}_\mathrm{s}(\mathbf{r})$ to point $\boldsymbol{r}$ in space [3, 9]. The superposition of $\mathbf{E}_\mathrm{s}(\mathbf{r})$ and $\mathbf{E}_\mathrm{i}(\mathbf{r}')$ changes the amplitude and phase of the signal received by the radio station, resulting in interference.

In the research of RRI from power transmission lines on AM radio station, Balmain and Belrose firstly found the resonance phenomenon [23], that is, at some frequency points, the power transmission lines suddenly cause great interference to the radio station, but at other frequency points, the interference is not obvious. In the subsequent study [6, 24], through measurements, Trueman and Kubina confirmed that the RRI was determined by the secondary radiation of the induced current generated by the power transmission lines under the irradiation of the external electromagnetic wave, and the frequency of the maximum induced current was the resonant frequency. Subsequently, based on antenna theory, IEEE determined the resonance mechanism and method for resonant frequency prediction and interference level measurement of RRI below 1.7 MHz.

When studying the protection distance between UHV lines and AM broadcasting stations in China [2], researchers also found the interference resonance phenomenon by calculating the RRI level from power transmission lines on the broadcasting stations in the range of 526.5 kHz~26.1 MHz, as shown in Figure 2. As can be observed from Figure 2, RRI still has resonance characteristics over 1.7 MHz, and the interference level is almost zero at some frequencies but higher at some other frequencies. Therefore, in order to suppress RRI over 1.7 MHz by avoiding the resonant frequencies, it is necessary to further study the resonance mechanism of RRI.

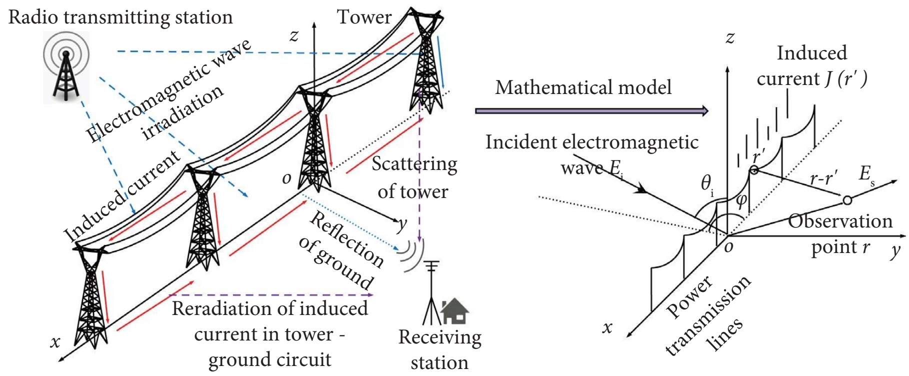

Figure 1: Model of RRI from power transmission lines on radio station.

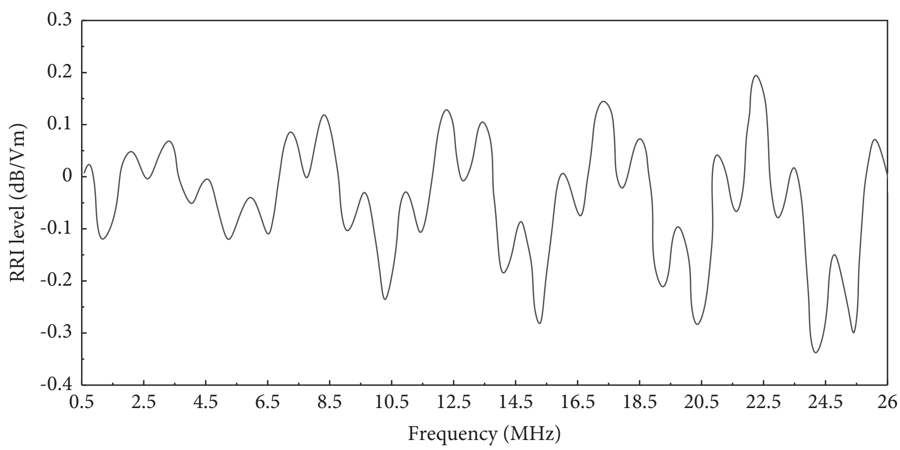

Figure 2: RRI level on AM broadcasting stations.

2.2. Study on RRI Resonance. According to the antenna theory, IEEE explains the resonance phenomenon of RRI in the following two situations, as shown in Figure 3. When the tower is connected with the ground wire, the two adjacent towers, the ground wire, and their ground image form a loop, which can be equivalent to a ring antenna; when the loop length is an integral multiple of the wavelength, the RRI resonance occurs due to standing wave phenomenon of induced current. When the tower is insulated from the ground wire, the interference is mainly caused by the tower. At this time, the tower and its ground image can be regarded as a half-wave antenna perpendicular to the ground; when the tower height is equal to $\lambda/4$, the induced current has an extreme value and generates RRI resonance.

It can be observed from Figure 3 that the premise for the IEEE guide is that the tower with complex structure must be equivalent to a single ideal line antenna with a certain radius. In this way, it is actually assumed that the induced current on the tower surface is distributed along the axis of the antenna. However, according to the recommendation of Numerical Electromagnics Code software, when the electric field integral equation is discretized, the length of the line element obtained by the line model subdivision should not exceed 0.1λ. With the increase of the incident electromagnetic wave frequency, the length of the split line element will decrease until its aspect ratio is too small, resulting in the assumption that the induced current of the ideal line antenna distributed along the axis is no longer valid. Therefore, the IEEE guide clearly indicates that its applicable frequency range does not exceed 1.7 MHz.

In the follow-up research [3], Tang et al. proposed a method for predicting the resonant frequency of RRI based on the generalized resonance theory, and the prediction range of the RRI resonance frequency is extended to 3 MHz for the first time. The key of this method is to construct the generalized system function of the electromagnetic open system composed of radio stations and power transmission lines, so as to predict the resonant frequency of the system by combining the zero-pole points describing the intrinsic characteristics of the system function and the quality factor Q value characterizing the energy storage of the system.

However, the generalized system function is actually obtained by interpolation in the complex frequency domain [3]. Therefore, the mathematical expression of the function depends on the interpolation condition, that is, the electric field intensity information at the observation point. When the electric field intensity information changes, the generalized system function will also change. Obviously, the generalized system function has nothing to do with the body structure of power transmission lines and cannot reflect the

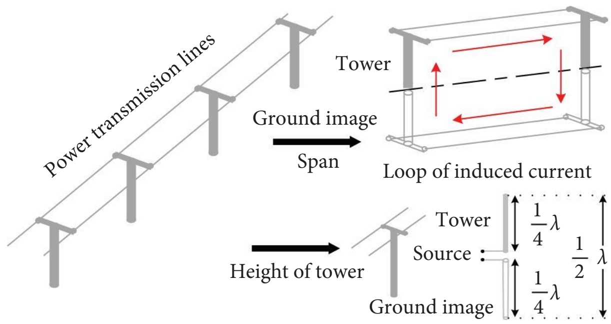

Figure 3: Equivalent model of RRI in IEEE guide.

intrinsic electromagnetic characteristics of power transmission lines, so it is impossible to clarify the correlation mechanism between RRI resonance and the body structure of power transmission lines.

Therefore, until now, scholars at home and abroad have not physically explained RRI resonance phenomenon of power transmission lines in the frequency band above 1.7 MHz. As a result, it is impossible to employ "detuning" technology to suppress RRI, and a large number of research can only focus on the formulation of RRI protection distance.

3. RRI Resonance Mechanism Analysis of Power Transmission Lines Based on CM Theory

3.1. Characteristic Current of Power Transmission Lines and Its Characteristics. The key of CM theory is to define a group of weighted orthogonal characteristic currents, so that the total induced current can be decomposed into linear superposition of the characteristic currents. According to the solution method of characteristic current for conducting body of arbitrary shape [19], the generalized eigenvalue equation for solving the characteristic current of power transmission lines can be directly given as

$$\mathbf{X}(\mathbf{J}_{\mathrm{n}}) = \upsilon_{\mathrm{n}}\mathbf{R}(\mathbf{J}_{\mathrm{n}}), \tag{1}$$

where $\mathbf{J}_n$ ($n = 1, 2, 3, \ldots, N$) is the nth-order characteristic current, υ_n is the eigenvalue corresponding to $\mathbf{J}_n$, and X and R are the imaginary part and the real part of the impedance operator Z, respectively. Z satisfies the following expression [7]:

$$\mathbf{Z}\left[\mathbf{J}\left(\mathbf{r}'\right)\right] = \left[j\omega\mu\int_{S'} G\left(\mathbf{r},\mathbf{r}'\right)\mathbf{J}\left(\mathbf{r}'\right)\mathrm{d}S' + \frac{j}{\omega\varepsilon}\nabla\int_{S'} G\left(\mathbf{r},\mathbf{r}'\right)\nabla'\cdot\mathbf{J}\left(\mathbf{r}'\right)\mathrm{d}S'\right]_{\tan}, \tag{2}$$

where $\mathbf{J}(\mathbf{r}')$ is the total induced current on the metal surface of power transmission lines, "tan" denotes the tangential component, ω is angular frequency, μ is permeability, ε is dielectric constant, and $G(\mathbf{r},\mathbf{r}')$ is Green's function in free space.

By using the numerical calculation method in [20], we can solve (1) and obtain the characteristic current $\mathbf{J}_{\mathrm{n}}$ and the corresponding eigenvalue υ_{n}.

From (1) and (2), it can be seen that the solution of $\mathbf{J}_{\mathrm{n}}$ is independent of external excitation. Therefore, $\mathbf{J}_{\mathrm{n}}$ can reflect the intrinsic distribution forms of the induced current on the metal surface of power transmission lines. Since the impedance operator used to construct the eigenvalue equation is a function of frequency, the amplitude and phase of $\mathbf{J}_{\mathrm{n}}$ will change with frequency. For the convenience of subsequent calculation, $\mathbf{J}_{\mathrm{n}}$ is normalized according to $\langle \mathbf{J}_{\mathrm{n}}, \mathbf{R}(\mathbf{J}_{\mathrm{n}})\rangle = 1$.

Also, any two characteristic currents $\mathbf{J}_{\mathrm{m}}$ and $\mathbf{J}_{\mathrm{n}}$ satisfy the following orthogonal relationship [19]:

$$\begin{cases} \langle \mathbf{J}_{\mathrm{m}}, \mathbf{R}(\mathbf{J}_{\mathrm{n}})\rangle = \langle \mathbf{J}_{\mathrm{m}}^{*}, \mathbf{R}(\mathbf{J}_{\mathrm{n}})\rangle = \delta_{\mathrm{mn}}, \\ \langle \mathbf{J}_{\mathrm{m}}, \mathbf{X}(\mathbf{J}_{\mathrm{n}})\rangle = \langle \mathbf{J}_{\mathrm{m}}^{*}, \mathbf{X}(\mathbf{J}_{\mathrm{n}})\rangle = \upsilon_{\mathrm{n}}\delta_{\mathrm{mn}}, \\ \langle \mathbf{J}_{\mathrm{m}}, \mathbf{Z}(\mathbf{J}_{\mathrm{n}})\rangle = \langle \mathbf{J}_{\mathrm{m}}^{*}, \mathbf{Z}(\mathbf{J}_{\mathrm{n}})\rangle = (1 + j\upsilon_{\mathrm{n}})\delta_{\mathrm{mn}}, \end{cases} \tag{3}$$

where " $*$ " represents conjugation.

3.2. The CM Radiation Characteristics of Power Transmission Lines. Based on the generalized eigenvalue equation, a set of characteristic currents and corresponding eigenvalues independent of external excitation have been solved in Section 3.1, which provides a basis for further study on the intrinsic electromagnetic characteristics of power transmission lines. Considering that RRI of power transmission lines is essentially the radiation, conversion, and storage of electromagnetic energy, and in combination with Poynting's theorem, this section further studies the radiation characteristics of CMs by explaining the physical meaning of υ_n.

Assume that the characteristic electric field and magnetic field generated by $\mathbf{J}_n$ of power transmission lines in the far field are $\mathbf{E}_n$ and $\mathbf{H}_n$, respectively. According to Poynting's theorem, there is the following energy relationship:

$$\begin{aligned} -\int_V \mathbf{J}_{\mathrm{n}}^{*}\cdot\mathbf{E}_{\mathrm{n}}\mathrm{d}v = &\int_{S_\infty}\left(\mathbf{E}_{\mathrm{n}}\times\mathbf{H}_{\mathrm{n}}^{*}\right)\cdot\hat{\mathbf{n}}\mathrm{d}S \\ &+ j\omega\int_V\left(\mu\left|\mathbf{H}_{\mathrm{n}}\right|^2 - \varepsilon\left|\mathbf{E}_{\mathrm{n}}\right|^2\right)\mathrm{d}v, \end{aligned} \tag{4}$$

where S_∞ represents the surface enclosing power transmission lines in Figure 1, V is the region enclosed by S_∞, and $\hat{\mathbf{n}}$ represents the unit normal vector on the surface S_∞.

According to the boundary conditions of the ideal conductor surface, $\mathbf{E}_n$ in $-\int_V \mathbf{J}_n^{*}\cdot\mathbf{E}_n\mathrm{d}v$ can be replaced with $-\mathbf{Z}(\mathbf{J}_n)$; therefore, (8) can be rewritten as

$$\begin{aligned} -\int_V \mathbf{J}_{\mathrm{n}}^{*}\cdot\mathbf{E}_{\mathrm{n}}\mathrm{d}v &= \int_V \mathbf{J}_{\mathrm{n}}^{*}\cdot\mathbf{Z}(\mathbf{J}_{\mathrm{n}})\mathrm{d}v \\ &= \langle \mathbf{J}_{\mathrm{n}}^{*}, \mathbf{R}(\mathbf{J}_{\mathrm{n}})\rangle + j\langle \mathbf{J}_{\mathrm{n}}^{*}, \mathbf{X}(\mathbf{J}_{\mathrm{n}})\rangle. \end{aligned} \tag{5}$$

Combining (3)–(5), the following expression can be derived:

$$\begin{cases} \langle \mathbf{J}_{\mathrm{n}}^{*}, \mathbf{R}(\mathbf{J}_{\mathrm{n}})\rangle = \int_{S_\infty} (\mathbf{E}_{\mathrm{n}} \times \mathbf{H}_{\mathrm{n}}^{*}) \cdot \hat{\mathbf{n}} \mathrm{d}S \\ \langle \mathbf{J}_{\mathrm{n}}^{*}, \mathbf{X}(\mathbf{J}_{\mathrm{n}})\rangle = \omega \int_{V} \left(\mu |\mathbf{H}_{\mathrm{n}}|^2 - \varepsilon |\mathbf{E}_{\mathrm{n}}|^2\right) \mathrm{d}v = v_{\mathrm{n}}, \end{cases} \tag{6}$$

where $\langle J_n^*, R(J_n)\rangle$ represents the electromagnetic energy radiated by the nth-order CM of power transmission lines. According to the precondition of $\langle J_n^*, R(J_n)\rangle = 1$, CM radiates unit power at any frequency.

The second item $\langle \mathbf{J}_n^*, \mathbf{X}(\mathbf{J}_n)\rangle$, namely, the eigenvalue v_n, denotes the electromagnetic energy stored in the nth-order CM of power transmission lines. Obviously, the smaller $|v_n|$, the less energy storage and the stronger the radiation ability of CM. When $|v_n|$ is 0, the energy stored is 0, that is, the energy radiated by CM reaches the maximum, so $v_n = 0$ is the RRI resonance condition for the nth-order CM of power transmission lines.

Hence, from the perspective of energy radiation, the RRI is associated with the intrinsic electromagnetic characteristics of the body structure of power transmission lines, which is independent of the observation points. For power transmission lines with fixed structure, v_n is only a function of frequency. According to (1), for different CMs, their resonant frequencies must be different. Therefore, calculating eigenvalue v_n provides a measure to find all the intrinsic resonant frequencies of power transmission lines in the frequency band.

Besides, combining the orthogonal relationship in (3) and energy relationship in (4), if $\mathrm{m} \neq \mathrm{n}$, the following relationship between the mth-order CM and the nth-order CM can be derived:

$$\begin{aligned} -\int_{V} \mathbf{J}_{\mathrm{m}}^{*} \cdot \mathbf{E}_{\mathrm{n}} \mathrm{d}v &= \int_{V} \mathbf{J}_{\mathrm{m}}^{*} \cdot \mathbf{Z}(\mathbf{J}_{\mathrm{n}}) \mathrm{d}v \\ &= (1 + \mathrm{j}v_{\mathrm{n}})\delta_{\mathrm{mn}} = 0. \end{aligned} \tag{7}$$

Equation (7) shows that the electric field $\mathbf{E}_n$ generated by the nth-order characteristic current $\mathbf{J}_n$ cannot drive the mth-order characteristic current $\mathbf{J}_m$. Therefore, any two CMs of power transmission lines are energy decoupling, that is, there is no electromagnetic energy exchange between any two CMs.

3.3. The Solution of CM-Related Parameters.

According to Section 3.1, under the irradiation of external electromagnetic wave, the induced current $\mathbf{J}(\mathbf{r}')$ on the metal surface of power transmission lines can be written as a superposition of the characteristic currents:

$$\mathbf{J}\left(\mathbf{r}'\right) = \sum_{\mathrm{n}=1}^{\mathrm{N}} \alpha_{\mathrm{n}} \mathbf{J}_{\mathrm{n}}, \tag{8}$$

where α_n is the coefficient of $\mathbf{J}(\mathbf{r}')$ expanded by $\mathbf{J}_n$, called modal weighting coefficient, which is related to external excitation and represents the contribution of $\mathbf{J}_n$ to the total induced current $\mathbf{J}(\mathbf{r}')$. Obviously, α_n will deeply influence the current induced on the surface of power transmission lines and determine which CMs will be the main mode that influences the energy radiated by power transmission lines indirectly. The expression of α_n can be written as [19]

$$\alpha_{\mathrm{n}} = \frac{\langle \mathbf{J}_{\mathrm{n}}, \mathbf{E}_{\mathrm{i}}\left(\mathbf{r}'\right)\rangle}{1 + \mathrm{j}v_{\mathrm{n}}}, \tag{9}$$

and from (9), two important CM parameters of power transmission lines are defined as

$$\begin{aligned} \mathrm{ME}_{\mathrm{n}} &= \langle \mathbf{J}_{\mathrm{n}}, \mathbf{E}_{\mathrm{i}}\left(\mathbf{r}'\right)\rangle, \\ \mathrm{MS}_{\mathrm{n}} &= \left|\frac{1}{1 + \mathrm{j}v_{\mathrm{n}}}\right|, \end{aligned} \tag{10}$$

where ME_n and MS_n are called modal excitation coefficient and modal significance, respectively. ME_n is related to specific external excitation and denotes the coupling degree between $\mathbf{J}_n$ and $\mathbf{E}_{\mathrm{i}}(\mathbf{r}')$, and it determines whether CM can be excited well by external excitation or not. MS_n is only related to v_n, namely, the intrinsic electromagnetic characteristics of power transmission lines. The value range of MS_n is [0, 1]. When $\mathrm{MS}_n = 1$, resonance of CM occurs, and it is more convenient to denote the radiation ability of CM with MS_n. Together with ME_n, MS_n determines the value of α_n. Obviously, CMs with high coupling degree and high MS_n value, namely, α_n with high value, can achieve more contribution to the total electromagnetic response caused by external excitation.

3.4. RRI Resonance Analysis Based on CM Theory.

Without specific external excitation, Section 3.3 analyzed the CM radiation characteristics of power transmission lines from the perspective of energy. However, considering that the external excitation may be coupled with multiple characteristic currents, that is, multiple CMs may be excited at the same time, the electromagnetic energy radiated by power transmission lines will no longer be determined by a single CM. It is unreasonable to take the intrinsic resonant frequencies of power transmission lines as the RRI resonance frequency. Therefore, in order to analyze RRI resonance of power transmission lines from the perspective of CM, we need to decompose the total energy radiated by power transmission lines into the superposition of energy radiated by each CM and then clarify the main CMs that influence the energy radiation of power transmission lines by using CM-related parameters.

The first item $\langle \mathbf{J}_n^*, \mathbf{R}(\mathbf{J}_n)\rangle$ in (6) gives the normalized form of energy radiated by CM. However, according to (8), $\mathbf{J}_n$ here is just used as a basis function to expand $\mathbf{J}(\mathbf{r}')$, and the real energy radiated under the specific external excitation is actually determined by modal weighting coefficient α_n. Replacing $\mathbf{J}_n$ in $\langle \mathbf{J}_n^*, \mathbf{R}(\mathbf{J}_n)\rangle$ with $\alpha_n \mathbf{J}_n$, the actual energy P_n radiated by the nth-order CM under specific external excitation can be written as

$$\begin{aligned} P_{\mathrm{n}} &= \langle \alpha_{\mathrm{n}} \mathbf{J}_{\mathrm{n}}^{*}, \mathbf{R}(\alpha_{\mathrm{n}} \mathbf{J}_{\mathrm{n}})\rangle \\ &= \alpha_{\mathrm{n}}{}^{2} \langle \mathbf{J}_{\mathrm{n}}^{*}, \mathbf{R}(\mathbf{J}_{\mathrm{n}})\rangle = \alpha_{\mathrm{n}}{}^{2}. \end{aligned} \tag{11}$$

According to (7), any two CMs of power transmission lines are energy decoupling; therefore, the total energy P_{total} radiated by power transmission lines can be expressed by the superposition of P_n as

$$P_{total} = \sum_{n=1}^{N} P_n = \sum_{n=1}^{N} \alpha_n{}^2. \tag{12}$$

As can be observed from (12), α_n can influence the energy radiated by power transmission lines and further influence the RRI resonance characteristics; hence, it is important to find out the CMs with high α_n, and these CMs may determine the RRI resonance of power transmission lines.

According to (9), α_n depends on ME_n and MS_n, and considering that ME_n is influenced by the external excitation, which may change with different radio stations in actual project, we firstly use half-power bandwidth criterion to find the significant CMs with $MS_n > 0.707$ [25], and these CMs have strong potential radiation ability. Those CMs with small or even 0 MS_n will give small α_n, and their potential contribution to the total energy radiated by power transmission lines must be very limited and can be ignored. Then, we can further consider the external excitation and calculate α_n of the significant CMs and finally analyze the RRI resonance of power transmission lines.

4. Simulation and Analysis

4.1. RRI Resonance Analysis of Power Transmission Lines below 1.7 MHz. When the frequency of external excitation is below 1.7 MHz, the cross-sectional size of the tower is far less than the wavelength of incident electromagnetic wave, so the details of the tower can be ignored Trueman et al. established a numerical model of a 500 kV double-circuit transmission line with V1S towers [6], as shown in Figure 4. The tower height is 50.9 m, and the span is 274 m. The tower and ground wire are equal to line model with equivalent radius of 3.51 m and 0.71 m, respectively. Study in [6] found that for power transmission lines composed of multiple spans, a representative span can be used for RRI calculation, and the RRI resonance characteristics are consistent with the measured results. So, in this paper, we also intend to take the representative span for RRI resonance analysis.

However, when studying the RRI, due to the existence of ground refraction and reflection, the ground will inevitably have an impact on RRI. Moreover, the complex ground conditions, including the fluctuation and different electromagnetic characteristics of the ground, will also have influences that cannot be ignored. In short, the ground cannot be neglected in the RRI resonance analysis. However, the above considerations are actually very complicated, and it is not the main work to deal with the influence of ground in this paper, so we adopt the same processing method as the IEEE guide in this paper, that is, we take the representative span and its ground image in Figure 4, namely, the electromagnetic structure composed of two iron towers, ground wires, and their ground images, for CM analysis.

The frequency responses of MS_n for the first six-order CMs are shown in Figure 5, and the other CMs with very small MS_n are ignored in the range of 0.3 MHz~1.7 MHz. Obviously, considering $MS_n > 0.707$, there are only four significant CMs, and the intrinsic resonant frequencies of power transmission lines are 0.47 MHz, 0.92 MHz, 1.29 MHz, and 1.62 MHz, corresponding to CM1, CM3, CM4, and CM5, respectively.

These four significant CMs may be well excited by external excitation, and according to (9) and (10), the other CMs with small modal significance will not make a great contribution to RRI, therefore only these four significant CMs can determine the RRI resonance of power transmission lines. Considering the spatial geometric distance between power transmission lines and the radio station in a wide-area space, the electromagnetic wave irradiated on power transmission lines can be regarded as a vertically polarized plane wave [2]. We calculated ME_n and α_n for the four significant CMs under the excitation of the vertically polarized plane wave (incident along the positive direction of the y-axis in Figure 4, with the amplitude of 1 V/m), and the frequency responses of ME_n and α_n are shown in Figures 6(a) and 6(b), respectively.

The results in Figure 6(b) show that under the excitation of vertically polarized plane wave, the contribution of CM3 and CM5 to the total electromagnetic response is almost 0, while CM1 and CM4 can show good radiation performance in this frequency band. In order to show which CMs mainly influence the radiation characteristics of power transmission lines, we calculated the energy radiated by CM1 and CM4 and the total radiation energy after their superposition. The normalized results are shown in Figure 6(c). From the maximum point of total radiation energy, the resonant frequencies of RRI are 0.47 MHz and 1.29 MHz. In order to further clearly show the dominant frequency band of effective radiation of each significant mode, we calculated the proportion of energy radiated by each CM ($\alpha_n{}^2/P_{total}$), and the results are shown in Figure 6(d). It can be observed that in 0.3 MHz~0.92 MHz, RRI resonance of power transmission lines depends on CM1, and in 0.92 MHz~1.7 MHz, it depends on CM4.

However, according to the resonance mechanism of "integral multiple wavelength loop resonance" proposed in IEEE guide (the loop length composed of representative span in Figure 4 is 751.6 m, and the formula for calculating resonant frequencies can be found in [4]), the RRI resonance frequencies below 1.7 MHz predicted by IEEE are 0.43 MHz, 0.86 MHz, and 1.29 MHz. The intrinsic resonant frequencies of power transmission lines obtained by CM theory, as shown in Figure 5, are indeed in good agreement with those resonant frequencies predicted by IEEE. However, these intrinsic resonant frequencies obtained by CM theory are independent of the external excitation; whether these intrinsic resonant frequency points can appear in RRI or not, the specific external excitation must be taken into consideration. When the power transmission lines are excited by vertically polarized plane wave, only CM1 and CM4 can show good radiation performance, resulting in the actual resonant

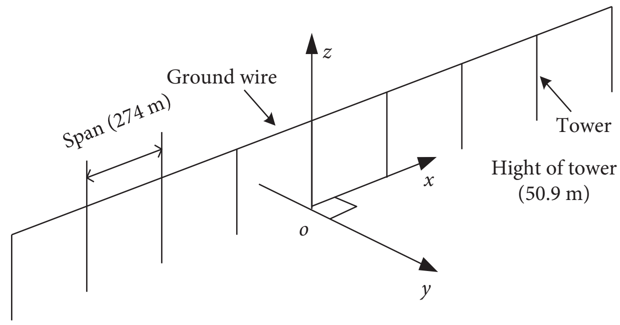

Figure 4: Model for RRI calculation of power transmission lines established by Trueman et al.

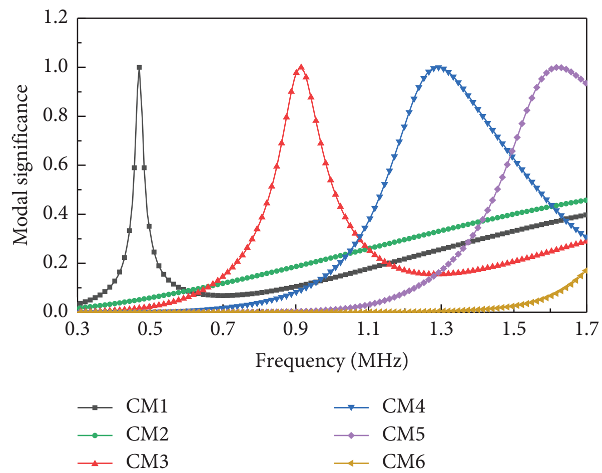

Figure 5: Frequency responses of MS_n below 1.7 MHz.

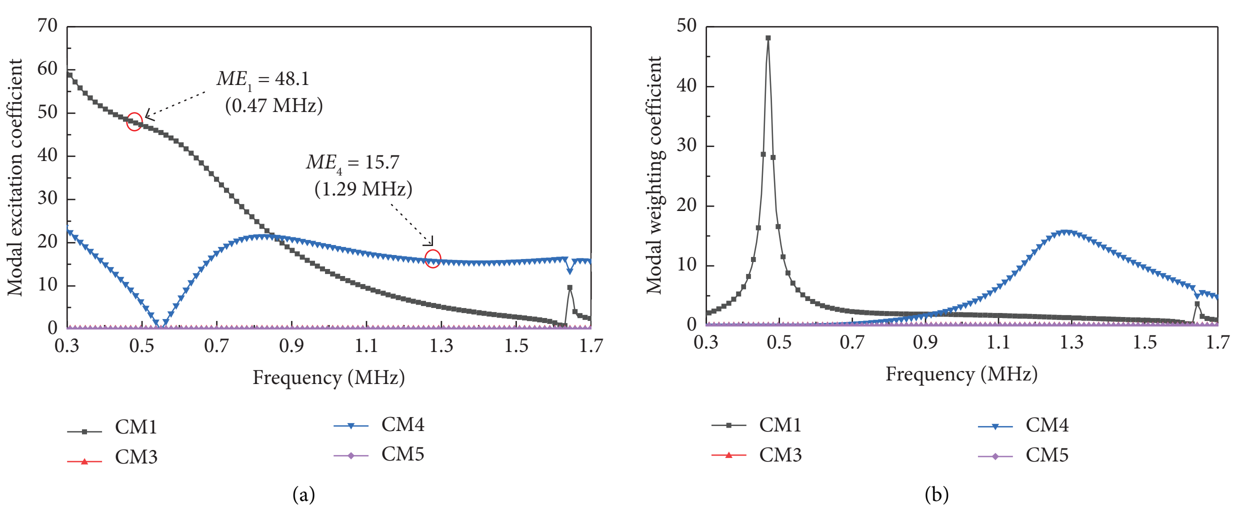

Figure 6: Continued.

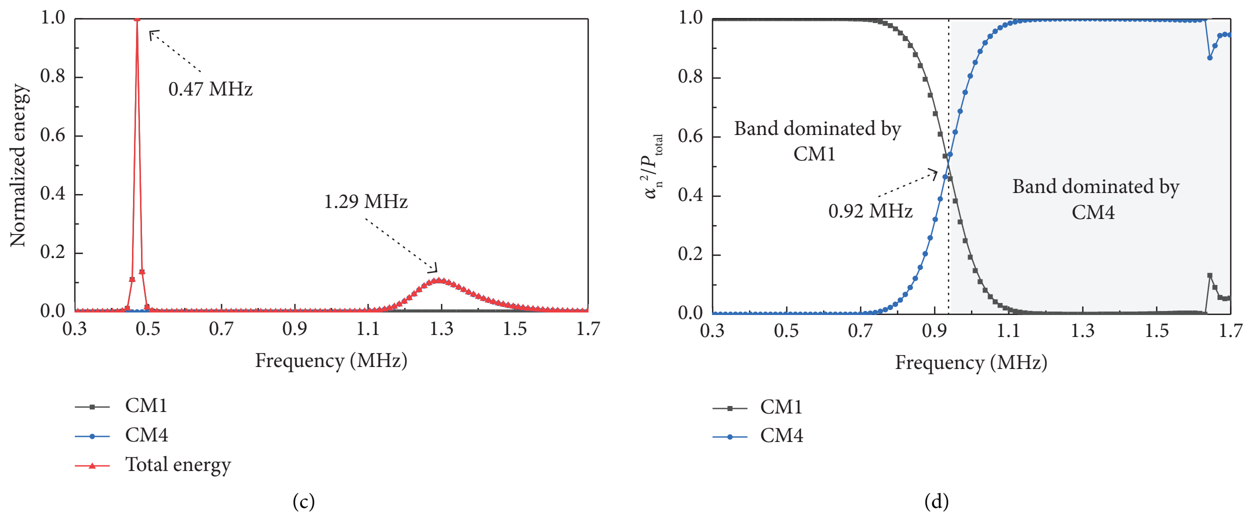

Figure 6: The related parameters for CM analysis of RRI below 1.7 MHz. (a) Modal excitation coefficient. (b) Modal weighting coefficient. (c) Normalized energy. (d) Proportion of energy radiated by each mode ($\alpha_n^2/P_{\text{total}}$).

frequencies being 0.47 MHz and 1.29 MHz, as shown in Figure 6(c). So, the analysis method based on CM theory actually does not give the resonant frequency of "double wavelength loop resonance," that is, the resonant frequency of 0.86 MHz disappears, and the results based on CM theory are consistent with those in [2]. From the perspective of CM, the reason for the results is that the vertically polarized plane wave cannot excite CM3 (the intrinsic resonant frequency of CM3 is near 0.86 MHz) and CM5, as shown in Figure 6(a), and the radiation of CM1 and CM4 at this frequency is also very weak. The specific analysis is as follows.

The characteristic current distribution of CM1, CM3, CM4, and CM5 is shown in Figure 7, respectively, where the arrow denotes the direction of the characteristic current on the subdivision element (the current on the subdivision unit with the same direction is indicated by the same arrow), and the colour depth represents the amplitude of characteristic currents.

Under the excitation of vertically polarized plane wave, each subdivision element of power transmission lines receives the same excitation. Because the current distributed along the axis on the overhead ground wire is orthogonal to the excitation, the interference of power transmission lines is mainly caused by the iron towers on both sides. The current direction of each subdivision element of the tower on both sides of CM1 and CM4 is the same. By solving (10), ME_1 is 48.1 at 0.47 MHz and ME_4 is 15.7 at 1.29 MHz, as shown in Figure 6(a). For CM3 and CM5, the current at the symmetrical positions of the two towers has the same amplitude but opposite direction, resulting in ME_3 and ME_5 being almost 0 under excitation of vertically polarized plane wave. Thus, even if the intrinsic resonant frequencies of CM3 and CM5 are in 0.3 MHz~1.7 MHz (namely, $\text{MS}_3 = 1$ and $\text{MS}_5 = 1$), CM3 and CM5 will not radiate energy and have no contribution to RRI (namely, $\alpha_3 = 0$ and $\alpha_5 = 0$). Finally, the resonant frequencies obtained by CM theory are 0.47 MHz and 1.29 MHz.

4.2. RRI Resonance Analysis of Power Transmission Lines in 1.7 MHz~3 MHz. When the frequency of external excitation exceeds 1.7 MHz, the tower details cannot be ignored relative to the electromagnetic wavelength, that is, the contribution of tower details to RRI is increasingly prominent. For this reason, based on the RRI model in [3] and considering that this paper is aimed at RRI in the medium-wave frequency band, a three-dimensional line model of power transmission lines that only considers the main materials of the tower is established, as shown in Figure 8, and the tower type is ZP30101, the tower height is 63 m, the cross arm is 41.2 m, and the span is 500 m.

Taking the representative span and its ground image for CM analysis, in 1.7 MHz~3 MHz, the first seven-order CMs are significant CMs, and the frequency responses of MS_n are shown in Figure 9.

The results show that 1.95 MHz, 2.15 MHz, 2.47 MHz, 2.70 MHz, 2.75 MHz 2.88 MHz, and 2.95 MHz are the intrinsic resonant frequencies of power transmission lines. We calculate ME_n, α_n, normalized radiation energy, and the proportion of energy radiated by each mode ($\alpha_n^2/P_{\text{total}}$) with the change of frequency under the excitation of vertically polarized plane wave. The results are shown in Figure 10.

From ME_n shown in Figure 10(a), we can conclude that the vertically polarized plane wave cannot well excite CM1, CM3, CM5, and CM7, resulting in the values of α_1, α_3, α_5, and α_7 being almost 0, as shown in Figure 10(b), namely, the contribution of CM1, CM3, CM5, and CM7 to RRI of power transmission lines is extremely limited in 1.7 MHz~3 MHz, so these four CMs can be ignored. RRI resonance in this frequency band mainly depends on CM2, CM4, and CM6. According to Figure 10(c), there are four maximum points of total radiation energy, namely, 2.30 MHz, 2.56 MHz, 2.85 MHz, and 3.0 MHz, which correspond to the RRI

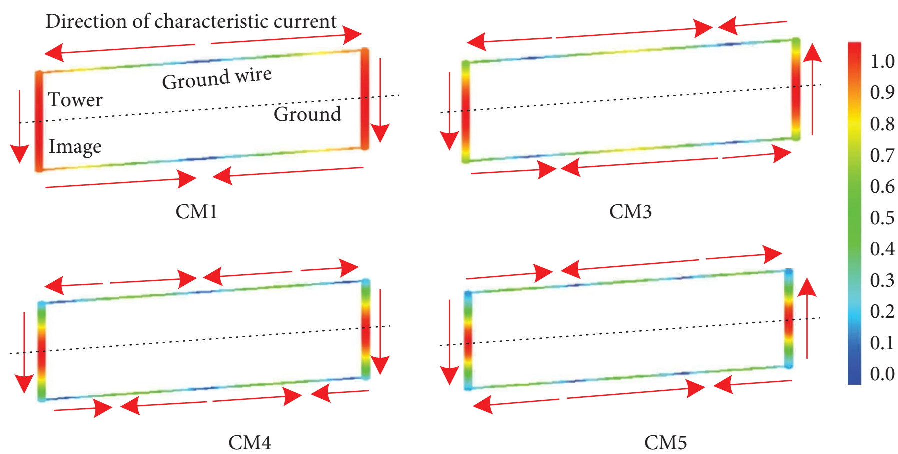

Figure 7: Characteristic currents for CM1, CM3, CM4, and CM5 below 1.7 MHz.

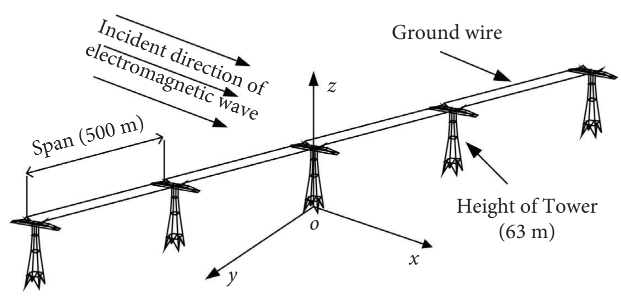

Figure 8: Three-dimensional line model of power transmission lines for RRI.

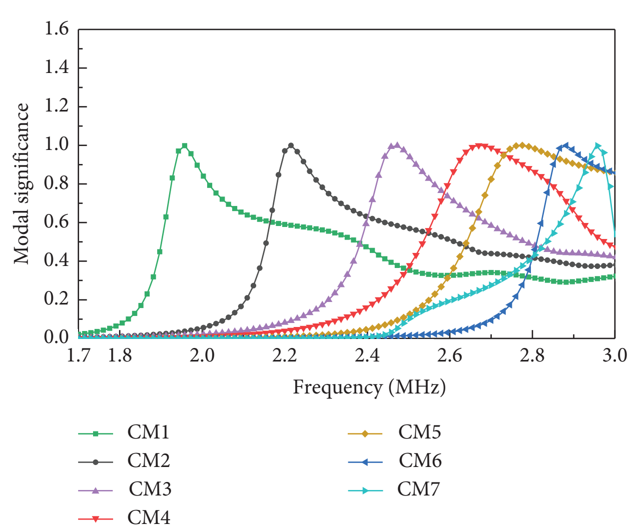

Figure 9: Frequency responses of MS_n in 1.7 MHz~3 MHz.

resonance frequencies. From Figure 10(d), it can be observed that in 1.7 MHz~2.69 MHz, RRI resonance mainly depends on CM2, in 2.65 MHz~2.88 MHz, it depends on CM4, and in 2.88 MHz~2.69 MHz, it depends on all three CMs.

Thus, the RRI resonance frequencies in 1.7 MHz~3 MHz are quite different from those, i.e., 2.03 MHz and 2.49 MHz, in [3]. The main reason for the deviation is that the method based on CM does not depend on the location of observation point and is related to the radiation energy of power transmission lines. However, the method based on the generalized resonance theory in [3] needs to construct the system function with the electric intensity information at the observation point. Obviously, the change of observation point will result in different system functions, and different RRI resonance frequencies will be obtained. To illustrate the problem, we translated the observation point, namely, (0,

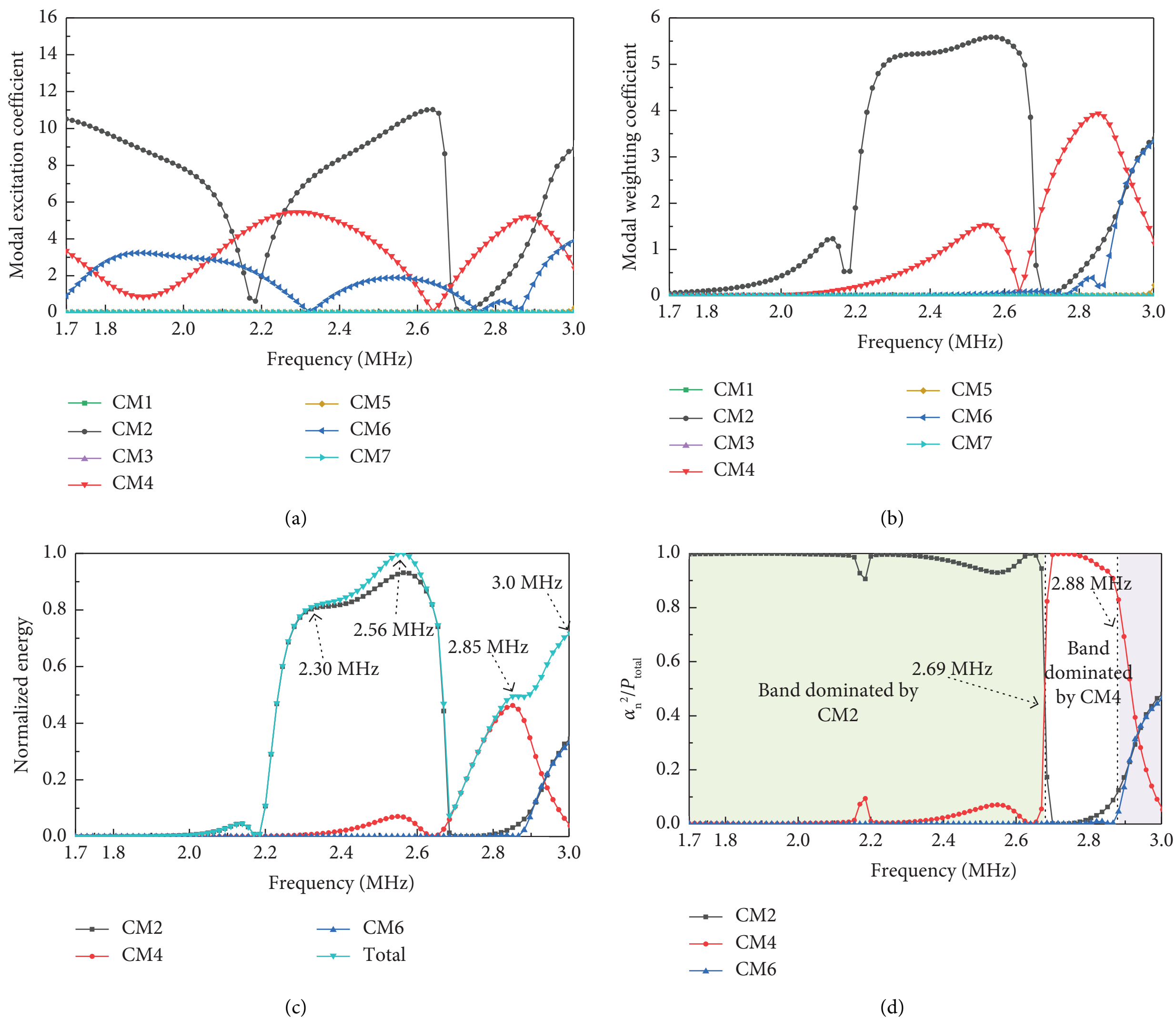

Figure 10: The related parameters for CM analysis of RRI in 1.7 MHz~3 MHz. (a) Modal excitation coefficient. (b) Modal weighting coefficient. (c) Normalized energy. (d) Proportion of energy radiated by each mode ($\alpha_n^2/P_{\text{total}}$).

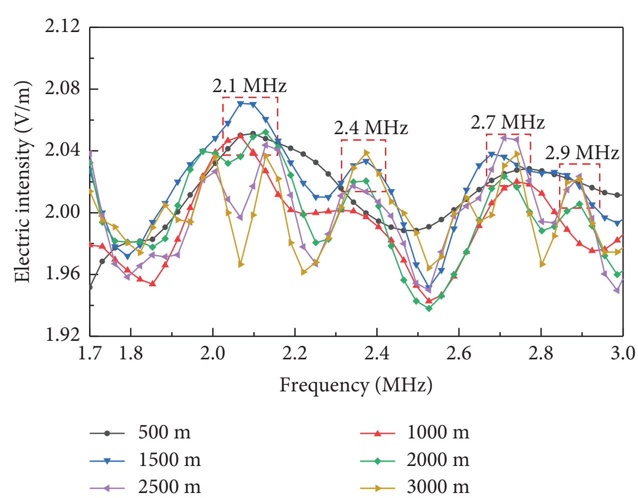

Figure 11: Frequency responses of electric intensity at different observation points.

2000 m, 2 m), in [3] along the x-axis to six different locations of (500 m, 2000 m, 2 m), (1000 m, 2000 m, 2 m), (1500 m, 2000 m, 2 m), (2000 m, 2000 m, 2 m), (2500 m, 2000 m, 2 m), and (3000 m, 2000 m, 2 m), and the frequency responses of the electric intensity are obtained by using the method in [3], and the results are shown in Figure 11.

As can be observed from Figure 11, the frequencies for the extreme value of electric intensity at six observation points are not exactly the same. But it is worth noting that the frequencies of the first four strongest electric intensities at six observation points are concentrated at about 2.1 MHz, 2.4 MHz, 2.7 MHz, and 2.9 MHz, as shown in the red rectangular boxes of Figure 11, which are in good agreement with the resonant frequencies based on CM analysis. To some extent, the comparison verifies the completeness of the method based on CM theory for RRI resonance analysis, and the method in this paper can clearly show all possible RRI resonance frequencies under specific external excitation.

5. Conclusions

(1) In order to clarify the RRI resonance mechanism of power transmission lines in medium-wave band, we introduced the CM theory into the study of RRI and proposed a method for RRI resonance analysis of power transmission lines based on CM theory. Comparing with IEEE guide and generalized resonance theory, the simulation results show that method proposed in this paper is reasonable and effective.

(2) The method proposed in this paper can reflect the intrinsic electromagnetic scattering characteristics of power transmission lines and does not depend on the location of the observation point. It can completely reflect the RRI resonance frequencies of power transmission lines and provide a theoretical support for the subsequent research on the suppression measures for RRI in medium-wave band.

(3) As mentioned in this paper, when the frequency exceeds 3 MHz, there still exists RRI resonance phenomenon. However, this paper mainly aims at the RRI resonance of power transmission lines in medium-wave band and uses simplified model of power transmission lines; when the frequency increases and the models are closer to real power transmission lines, the dimension of matrix for solving the generalized eigenvalue equation based on the Method of Moments (MoM) will become large, resulting in more CMs and difficulties for CM analysis of RRI resonance. Therefore, further research is needed on RRI.

Data Availability

The simulation data used to support the findings of this study are available from the corresponding author upon reasonable request.

Disclosure

This work is a further study of our early conference paper published in the following link: https://ieeexplore.ieee.org/document/9960365. We made a report about our rough ideas on this work when attending the conference and received good comments from the experts. In this paper, we have made the following improvements. (1) We have completely deduced the characteristic mode theory based on the electric field integral equation of the power transmission lines, and the related parameters also have been solved and explained. (2) We derived the mathematical expression of the energy radiated by each characteristic mode and verified the decoupling characteristics of energy radiated by any two modes, so the total energy can be written as the superposition of energy radiated by each mode. But we simply used modal weighting coefficient as the electromagnetic response in the conference paper, which seems inaccurate now, even though the simulation results seem correct. (3) We extended the frequency to 3 MHz with more precise model of power transmission lines, namely, work in this paper covers the whole medium-wave band, while the conference paper is only limited to 1.7 MHz.

Conflicts of Interest

The authors declare that they have no conflicts of interest.

Acknowledgments

This study was supported by Joint Funds of the National Natural Science Foundation of China under grant no. U20A20305. The authors would like to thank Dr. Gan from China Electric Power Research Institute for his early efforts on this work.

References

[1] C. W. Trueman, S. J. Kubina, R. C. Madge, and D. E. Jones, “Comparison of computed RF current flow on a power line with full scale measurements,” *IEEE Transactions on Broadcasting*, vol. 30, no. 3, pp. 97–107, 1984.

[2] B. Tang, Y. F. Wen, X. W. Zhang, and Z. B. Zhao, “Key problems of solving reradiation interference protecting distance between power transmission line and radio station at MF and SF,” *Proceedings of the CSEE*, vol. 31, no. 19, pp. 129–137, 2011.

[3] B. Tang, B. Chen, Z. B. Zhao, Z. Xiao, and S. Wang, “Resonance frequency estimation of reradiation interference at MF from power transmission lines based on generalized resonance theory,” *Journal of Electrical Engineering and Technology*, vol. 10, no. 3, pp. 1144–1153, 2015.

[4] IEEE, “IEEE guide on the prediction, measurement, and analysis of AM broadcast reradiation by power lines,” *IEEE Standard*, vol. 1260, 1996.

[5] C. W. Trueman and S. J. Kubina, “Numerical computation of the reradiation from power lines at MF frequencies,” *IEEE Transactions on Broadcasting*, vol. 27, no. 2, pp. 39–45, Jun. 1981.

[6] C. W. Trueman, S. J. Kubina, and J. S. Belrose, "Corrective measures for minimizing the interaction of power lines with MF broadcast antennas," *IEEE Transactions on Electromagnetic Compatibility*, vol. 25, no. 3, pp. 329–339, 1983.
[7] T. Bo, W. Yuanfang, Z. Zhibin, and Z. Xiaowu, "Computation model of the reradiation interference protecting distance between radio station and UHV power lines," *IEEE Transactions on Power Delivery*, vol. 26, no. 2, pp. 1092–1100, 2011.
[8] J. Zou, F. Wu, L. Jiang, F. P. Wang, and R. J. Tan, "Study on calculation of passive Interference of HVDC transmission line to short-wave radio direction station with spatial spectral estimation direction finding algorithm," *Power System Technology*, vol. 44, no. 4, pp. 1582–1588, 2020.
[9] Z. B. Zhao, Z. Y. Gan, X. W. Zhang, X. Cui, and X. Wu, "Passive interference to radio station caused by UHV AC transmission line in short wave frequency," *High Voltage Engineering*, vol. 35, no. 8, pp. 1818–1823, 2009.
[10] X. W. Zhang, X. F. Liu, X. Wu, B. Q. Wan, and G. Z. Zhang, "Calculation of radio interference from HV AC transmission line to aeronautical radio navigation," *High Voltage Engineering*, vol. 35, no. 8, pp. 1830–1835, 2009.
[11] P. Zhao, J. S. Zhu, Y. M. Han, and X. D. Qu, "Protection distance for short wave frequency direction-finding station to reduce passive interference caused by transmission lines," *Power System Technology*, vol. 36, no. 5, pp. 22–28, 2012.
[12] B. Tang, H. T. Jiang, H. Y. Cao, R. Sun, and R. Liu, "Resonant frequency evaluation on reradiation interference from power transmission line based on the generalized resonance," *IEEE Transactions on Applied Superconductivity*, vol. 26, no. 7, pp. 1–5, 2016.
[13] B. Tang, H. Y. Cao, S. Wang, Y. X. Peng, and Y. Li, "Resonance frequency prediction of reradiation interference from power lines in medium wave band based on the generalized resonance," *Journal of Chongqing University*, vol. 39, no. 6, pp. 101–110, 2016.
[14] L. Li, H. X. Liu, Y. Shi, and C. H. Liang, "Generalized system function analysis of resonance behavior of electromagnetic open systems," *Science in China, Series A: Information Sciences*, vol. 35, no. 10, pp. 1096–1110, 2005.
[15] E. Antonino-Daviu, M. Cabedo-Fabrés, M. Sonkki, N. Mohamed Mohamed-Hicho, and M. Ferrando-Bataller, "Design guidelines for the excitation of characteristic modes in slotted planar structures," *IEEE Transactions on Antennas and Propagation*, vol. 64, no. 12, pp. 5020–5029, 2016.
[16] Y. Shi, Z. K. Meng, W. Y. Wei, W. Zheng, and L. Li, "Characteristic mode cancellation method and its application for antenna RCS reduction," *IEEE Antennas and Wireless Propagation Letters*, vol. 18, no. 9, pp. 1784–1788, 2019.
[17] S. Ghosal, A. De, A. P. Duffy, and A. Chakrabarty, "Selection of dominant characteristic modes," *IEEE Transactions on Electromagnetic Compatibility*, vol. 62, no. 2, pp. 451–460, 2020.
[18] P. Ylä-Oijala and H. Wallén, "PMCHWT-Based characteristic mode formulations for material bodies," *IEEE Transactions on Antennas and Propagation*, vol. 68, no. 3, pp. 2158–2165, 2020.
[19] R. F. Harrington and J. R. Mautz, "Theory of characteristic modes for conducting bodies," *IEEE Transactions on Antennas and Propagation*, vol. 19, no. 5, pp. 622–628, 1971.
[20] R. F. Harrington and J. R. Mautz, "Computation of characteristic modes for conducting bodies," *IEEE Transactions on Antennas and Propagation*, vol. 19, no. 5, pp. 629–639, 1971.
[21] I. Tzanidis, K. Sertel, and J. L. Volakis, "Characteristic excitation taper for ultrawideband tightly coupled antenna arrays," *IEEE Transactions on Antennas and Propagation*, vol. 60, no. 4, pp. 1777–1784, 2012.
[22] Y. Chen, "Alternative surface integral equation-based characteristic mode analysis of dielectric resonator antennas," *IET Microwaves, Antennas and Propagation*, vol. 10, no. 2, pp. 193–201, 2016.
[23] K. G. Balmain and J. S. Belrose, "AM Broadcast Reradiation from Buildings and Power Lines," in *Proceedings of the Electric Engineering Institution Conference*, pp. 268–272, Petersburg, Russia, October 1978.
[24] C. W. Trueman and S. J. Kubina, "Power line tower models above 1000 kHz in the standard broadcast band kHz in the standard broadcast band," *IEEE Transactions on Broadcasting*, vol. 36, no. 3, pp. 207–218, 1990.
[25] C. Wang, Y. Chen, and S. Yang, "In-band scattering reduction for a U-slot patch antenna," *IEEE Antennas and Wireless Propagation Letters*, vol. 19, no. 2, pp. 312–316, 2020.